International Journal of Nanoelectronics and Materials
IJNeaM
ISSN 1985-5761 | E-ISSN 2232-1535

Nanotechnology-based Implantable Drug Delivery: Characterization of Electrospun Temozolomide-Cellulose Acetate Nanofibers

Asyikin Sasha Mohd Hanif[a], Renatha Jiffrin[b], Siti Ernieyanti Hashim[c], Saravana Kumar Jaganathan[d], and Mohamad Ikhwan Jamaludin[b,*]

[a]*Malaysia-Japan International Institute of Technology, Universiti Teknologi Malaysia, Kuala Lumpur, 54100, Malaysia*
[b]*Bioinspired Device and Tissue Engineering Research Group, Department of Biomedical Engineering and Health Sciences, Faculty of Electrical Engineering, Universiti Teknologi Malaysia, Johor Bahru, 81310, Malaysia*
[c]*Department of Chemistry, Faculty of Science, Universiti Teknologi Malaysia, Johor Bahru, 81310, Malaysia*
[d]*Biomedical Engineering Research Group, School of Engineering, University of Leicester, University Road, Leicester, LE1 7RH, United Kingdom*
** Corresponding author. Tel.: +6019-6106905; e-mail: mohamad.ikhwan@utm.my*

Received 15 June 2025, Revised 15 Aug 2025, Accepted 21 May 2026

ABSTRACT

Electrospinning is a promising nanotechnology-based method for fabricating drug-loaded nanofibers. In implantable drug delivery systems (IDDS), electrospun nanofibers can offer targeted and sustained drug release owing to their high surface area-to-volume ratio, tunable porosity, and ability to incorporate various therapeutic agents. This study describes the preparation of electrospun cellulose acetate (CA) nanofibers as sophisticated biomaterials loaded with temozolomide (TMZ), a widely used anticancer drug for treating brain tumors. CA nanofibers loaded with TMZ were synthesized by electrospinning CA at a constant concentration of 17% (w/v) and different TMZ loadings (5 mg, 10 mg, and 15 mg). Electrospun TMZ–CA nanofiber membranes were characterized by scanning electron microscopy (SEM), Fourier-transform infrared spectroscopy (FTIR), and ultraviolet-visible spectrophotometer (UV-Vis). SEM analysis confirmed uniform, bead-free fibers with increasing diameter as TMZ concentration increased. FTIR and UV-Vis spectroscopy analysis confirmed that TMZ retained its stability and molecular integrity within the CA matrix following fabrication. In addition, sessile drop contact angle studies indicated hydrophobicity, consistent with continued drug release. As TMZ loading increased, the tensile modulus, tensile strength, and elongation at break decreased, reflecting drug disruption in the polymer matrix. In vitro drug release studies revealed a biphasic profile, with 22-26% of the drug released within 8 hours, indicating sustained delivery potential. The cytotoxicity study showed that higher TMZ loading increased and sustained tumor cell killing. This work highlights the effectiveness of electrospinning as a fabrication technique to produce structurally stable, drug-loaded nanofibers, emphasizing their potential as implantable systems for localized chemotherapy.

Keywords: *Electrospinning, Glioblastoma, Implantable drug delivery, In vitro drug release, Nanofibers*

1. INTRODUCTION

The advancement of sophisticated biomaterials is necessary for the progress of modern drug delivery systems (DDS), especially in the treatment of aggressive cancers. Among these materials is a biocompatible and biodegradable cellulose derivative, cellulose acetate (CA), which has attracted considerable interest due to its mechanical properties, ease of processing, and structural flexibility. These properties make CA an attractive candidate for developing implantable drug delivery platforms, such as processed nanofibrous scaffolds [1-4].

Electrospinning is an innovative and scalable fabrication technique that can transform CA into nanofiber structures that mimic the extracellular matrix (ECM). Electrospun CA nanofibers have a high surface area-to-volume ratio, and their porosity and drug-loading capacity can be controlled. These characteristics enable both localized and sustained drug release, making them excellent for targeted chemotherapy applications [5-6].

With one of the most malignant forms of brain tumors with low survival rates, glioblastoma multiforme (GBM), strategies for modifying suitable material are crucial. Conventional routes of drug administration by either oral or intravenous are typically associated with significant systemic side effects resulting from the generic biodistribution of the drug delivery system and the unpredictable drug release properties, especially when used to treat aggressive types of cancer [7].

Temozolomide (TMZ) has been widely accepted as a chemotherapeutic agent primarily used to treat GBM, owing to its ability to cross the blood-brain barrier (BBB) and induce damage to tumor DNA, resulting in apoptosis [8]. Although TMZ is highly effective in treating GBM as a first-line chemotherapeutic agent, it also presents several limitations to its use, including rapid hydrolysis of TMZ at physiological pH values, poor and unpredictable drug distribution within the body, systemic toxicity, and mechanisms of drug resistance developed in the tumor cells [9-10]. Therefore, the development of novel DDS is essential to improve the efficacy of TMZ therapy through sustained release of TMZ at the tumor site.

This study highlights the fabrication and characterization of electrospun CA nanofibers loaded with TMZ and the evaluation of their physicochemical properties, structural integrity, and potential for sustained, implantable drug release tailored for glioblastoma treatment.

2. MATERIALS AND METHODS

2.1. Materials

The materials used in this work are cellulose acetate (CA) (Sigma-Aldrich, Mn = 30,000, 39.8 wt% acetyl), temozolomide (TMZ, Tokyo Chemical Industry), acetone (Sigma-Aldrich, 99.5%), ethanol (Sigma-Aldrich, 99.5%), N-dimethylacetamide (DMAc, Sigma-Aldrich, 99%), phosphate-buffered saline (PBS, pH 7.4) (ThermoFisher), and Tube-O-dialysis membrane (Sigma-Aldrich, MWCO 1 kDa).

2.2. Preparation of Nanofiber Solutions

The preparation of CA/TMZ solutions was adapted from a previous study [11]. CA powder was dissolved in a ternary solvent mixture of acetone, DMAc, and ethanol at a 3:2:1 (v/v) ratio and stirred for 6 hours to obtain a homogeneous CA solution at 17% w/v. TMZ was added at three concentrations (5 mg, 10 mg, 15 mg) to separate aliquots, and the mixtures were stirred for another 4 hours to obtain homogeneous CA/TMZ blended solutions [12]. All solutions were freshly prepared before the electrospinning process to prevent TMZ instability and degradation [13-14].

2.3. Electrospinning Process

A nanofiber mat was developed from the prepared solution via electrospinning, as illustrated in Figure 1. Each solution was filled into a 5-ml syringe with a 23-gauge needle with a flattened tip. The needle tip was clipped to a positive-voltage source, with the tip-to-metal collector distance fixed at 12 cm. The collector was wrapped in aluminum foil and maintained at a constant negative voltage of 11 kV. The solution was dispensed under a constant flow rate of 0.5 mL/h and electrospun at ambient temperature.

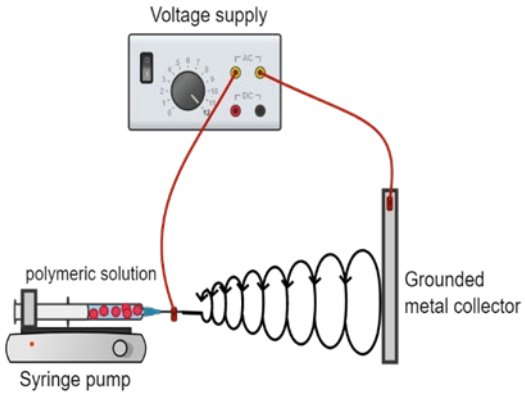

Figure 1. Schematic diagram of the electrospinning process.

2.4. Characterizations

2.4.1. Morphological Characterization

The morphology of the obtained electrospun mats was observed using scanning electron microscopy (SEM; Hitachi TM-3000). Before imaging, samples were platinum-coated for 4 min at 10 mA using a Quorum Q150R Thin Film Coater to prevent charging during scanning.

2.4.2. Chemical Composition of Electrospun Nanofibers

To examine the functional groups of the polymer and the polymer-drug interaction, a Fourier transform infrared spectrometer (FTIR Spectrum ONE, PerkinElmer) was used in combination with a single ATR platinum reflection diamond sampling module. Before obtaining the sample spectrum, a baseline spectrum was collected and subtracted from the sample spectrum. The spectra were then analyzed at a resolution of 4 cm^{-1} over the wavenumber range 650-4000 cm^{-1} [15].

2.4.3. Surface Wettability Measurement

The surface wettability of the electrospun nanofiber mat was assessed using the sessile drop technique and snapshots of the contact angle system (VCA Optima, AST Products, Inc.). A 5 µL droplet of distilled water was placed on the fiber surface, and images were captured immediately.

2.4.4. Tensile Measurement

An Instron machine was used to test the mechanical properties of the electrospun nanofibers. The protocol was referred to the ASTM standard (ASTM D882-10). This tester can be used for small- to medium-specimen elongation with a force range of 30 kN. The sample was cut into 10 × 25 mm strips before being mounted on the tensile tester's grips. The sample was then pulled until failure within the force range of 0.5-50 N. The obtained stress-strain graph was used to determine Young's modulus, tensile strength, and elongation at break.

2.4.5. In Vitro Drug Release of TMZ

The nanofiber membrane's capacity to release TMZ was determined using dynamic dialysis, where the fibrous membrane (100 mg) was placed in a dialysis tube (1 kDa molecular weight cut-off) containing 5 mL of PBS. The tube was suspended in a beaker containing 100 mL of PBS and 2% ethanol. The beaker was placed in a shaker at a speed of 80 rev/min at a temperature of 37 °C. At different time points, 3 mL of release medium was withdrawn from the beaker. To maintain the volume of medium in the beaker, the same amount of PBS solution was added after every withdrawal. The extracted medium was then put into an ultraviolet-visible (UV-Vis) spectrophotometer (Genesys 10S UV-Vis, Thermo Scientific) to measure the amount of TMZ released into the medium. The absorption peak of 328 nm was used to calculate the drug release. The drug release concentration was determined on the calibration curve of TMZ and the determined amount of electrospun nanofibers. The concentration is usually expressed as:

$$Concentration\ \left(\frac{mg}{mL}\right) = \frac{Amount\ of\ drug\ (mg)}{Volume\ of\ solution\ (mL)}$$

2.4.6. Cytotoxicity Study of Electrospun Nanofibers

The cell cytotoxicity of the electrospun nanofibers was assessed with the U-87 MG human GBM cell line using the MTT assay. The GBM cell was first cultured in culture flasks with Dulbecco's Modified Eagle Medium (DMEM), 10% fetal bovine serum (FBS), and 1% penicillin-streptomycin. The flasks were placed in an incubator maintained in a humidified environment containing 5% CO_2 at 37 °C. Before this, extract solutions were prepared from the electrospun nanofibers. The nanofibers were placed in a complete culture medium and incubated for 24-48 hours. The extracts were then filtered using a 0.22 µm sterile syringe filter.

The harvested GBM cells from the culture flask were seeded in a 96-well plate containing 3 × 10^4 cells/ well. After 24 hours of incubation, the medium was removed and replaced with different treatment groups: blank (no cells), negative control (cells only), and experimental group (CA and CA-TMZ extracts). The plates were incubated for 7 days, with fresh medium replaced every 48 hours. For the cytotoxicity study, the MTT powder was first dissolved in phosphate-buffered saline (PBS) to a concentration of 5 mg/mL. The MTT solution was placed in the well plate after the medium was discarded and replaced with fresh medium. The well plate was incubated for 4 hours to allow viable cells to reduce MTT to formazan crystals. The medium, together with MTT, was removed, and 150 µL of dimethyl sulfoxide (DMSO) was added to each well to dissolve formazan crystals. For complete dissolution, the plate was shaken for 10 min before the absorbance of each well was measured at 570 nm using a microplate reader (Tecan Infinite M200 PRO). The experiment was repeated for 1, 3, 5, and 7 days of cell incubation.

3. RESULTS

3.1. Morphological Characterization

Figure 2 displays the SEM images of electrospun CA and CA/TMZ nanofiber mats. All SEM images revealed nanofibers with smooth, uniform, and cylindrical structures. The fibers were arranged in a randomly oriented and interconnected network. The pristine CA fibers ranged between 100 and 300 nm. With the incorporation of TMZ, the fiber diameter increased with increasing TMZ concentration, likely due to higher solution viscosity [16]. The fiber diameter ranges for CA/TMZ5, CA/TMZ10, and CA/TMZ15 were 180-350, 220-400, and 250-450 nm, respectively. Despite increasing in size, the fibers retained consistent morphology, indicating stability during electrospinning and effective drug incorporation [17-18].

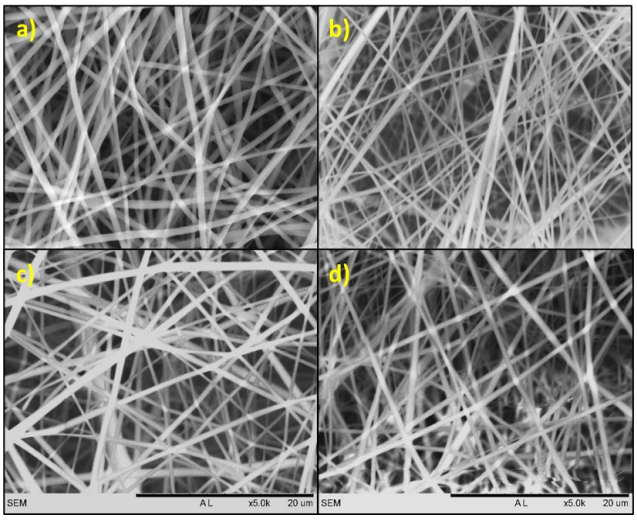

Figure 2. SEM images of (a) CA, (b) CA/TMZ5, (c) CA/TMZ10, and (d) CA/TMZ15 nanofibers. The scale bar represents 20 µm.

3.2. FTIR Analysis

To compare the spectra, pristine electrospun CA was used as a control sample against TMZ of different weights integrated with CA, as depicted in Figure 3. The FTIR spectra studies demonstrated chemical bond peaks involving the active component of the CA polymer and TMZ. The prominent, broad peak observed for pristine CA at 3461.71 cm^{-1} was attributed to the stretching vibrations of the O–H group [19]. Whilst in 5, 10, and 15 mg of TMZ, the spectra were shifted to 3474.37 cm-1, 3478.04 cm-1, and 3482.33 cm-1, respectively. This shift may be attributed to the interaction between the CA polymer and TMZ, which alters the hydrogen-bonding environment of the OH groups.

The peaks at 2944.16 cm-1 and 2887.56 cm-1 indicate methyl groups -CH- bond stretching correspondingly [19]. However, in the FTIR spectra of CA/TMZ nanofiber mat, these peaks were displaced to 2946.58cm^{-1} and 2889.16cm^{-1} for CA/TMZ5, 2946.31cm^{-1} and 2886.21cm^{-1} for CA/TMZ10, and 2946.08cm^{-1} and 2887.40cm^{-1} for CA/TMZ15. The carbonyl group C=O stretching vibration at 1737.90 cm-1 in pristine CA has been shifted to 1737.68 cm-1 in CA/TMZ5, 1737.92 cm-1 in CA/TMZ10, and 1740.08 cm^{-1} in CA/TMZ15, with little difference in the spectral shifts. The -CH_2- deformation vibration at 1429.43 cm-1 for pristine CA has been shifted to 1431.73 cm-1 for CA/TMZ5 and CA/TMZ10, and to 1431.97 cm-1 for CA/TMZ15 mat. The interaction of CA with TMZ was confirmed by widening peaks at 1034-1228cm^{-1} due to overlapping simple peaks. The C-O-C stretching vibration in pristine CA, initially at a spectrum of 1034.88 cm-1, has been shifted to 1035.74 cm^{-1}, 1035.87 cm^{-1}, and 1039.01 cm^{-1} for CA/TMZ5, CA/TMZ10, and CA/TMZ15, respectively.

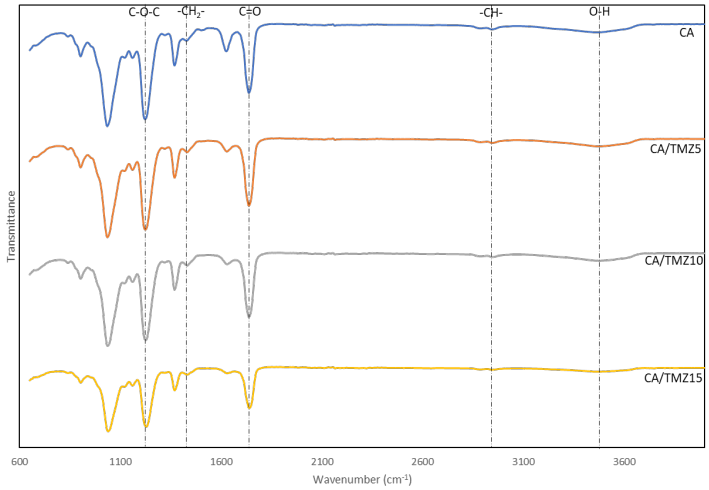

Figure 3. FTIR spectra of CA and CA/TMZ nanofibers.

3.3. Surface Wettability

Surface wettability of electrospun CA nanofibers containing different TMZ concentrations was evaluated using water contact angle (WCA) measurements, as detailed in Table 1. The WCA values offer valuable information about the hydrophilic or hydrophobic nature of the nanofiber surfaces, which plays a critical role in their interaction with aqueous environments - an essential factor in drug delivery applications. Pristine CA nanofibers showed a moderately hydrophobic surface with an average WCA of 128.26° [20]. As TMZ loading increased, the contact angle gradually increased, reaching 136.36° at the highest loading of 15 mg. This upward trend suggests that higher TMZ concentrations enhance the surface hydrophobicity of the nanofibers.

Table 1 Water contact angle of electrospun CA and CA/TMZ nanofibers

Sample name	Mean ± standard deviation of WCA (°)
CA	128.26 ± 1.12
CA/TMZ5	134.00 ± 0.99
CA/TMZ10	135.70 ± 0.58
CA/TMZ15	136.36 ± 0.97

3.4. Structural Integrity and Mechanical Properties

The mechanical properties of the nanofibers made via electrospinning are defined by Young's modulus, ultimate tensile strength, and percent elongation at break as summarized in Table 2. The results of the mechanical testing of pristine CA nanofiber had a tensile modulus of 0.65 MPA. The tensile modulus gradually decreased as TMZ loading increased, yielding values of 0.64, 0.57, and 0.47 MPa. The decrease in tensile modulus indicates that the addition of TMZ reduced the stiffness of the nanofibers. The tensile strength decreased from 2.33 MPa for pristine CA to 1.74 MPa for CA/TMZ15, indicating a loss of mechanical integrity as the drug concentration increased. In addition to

a decrease in tensile strength, there is a decrease in elongation at break from 21.12% for pristine CA to 18.96% for CA/TMZ15, which may indicate a slight loss of ductility due to reduced flexibility with the inclusion of TMZ [21].

Table 2 Mechanical properties of electrospun CA and CA/TMZ nanofibers

Sample name	Tensile Modulus (MPa)	Tensile Strength (MPa)	Elongation at Break (%)
CA	0.65	2.33	21.12
CA/TMZ5	0.64	2.21	20.02
CA/TMZ10	0.57	2.02	19.97
CA/TMZ15	0.47	1.74	18.96

3.5. In Vitro Drug Release of TMZ

Graph 4 shows the in vitro drug release profile of TMZ at different concentrations over the evaluation period. The profiles proved the importance of the drug-polymer interaction. To obtain a proper release profile, it was first necessary to obtain a calibration curve for the drug, in which absorbance values were plotted against the standard concentrations of the drug from 5–100 µg/mL. The calibration curve was linear, indicating that as the absorbance of the drug solution increased, the drug concentration increased proportionally, consistent with the Beer-Lambert law. The slight positive intercept was probably due to baseline absorbance or instrumental error, which is inherent in all spectrophotometer readings. Thus, from this linearity, the UV-Vis. A spectrophotometric detection method for accurate quantification of the drug in solution has been validated [22]. The calibration curve equation, along with its high coefficient of determination (R^2), confirmed that absorbance measurements can reliably quantify unknown TMZ concentrations in future formulation or drug release studies. This calibration step is vital in determining the drug loading and assessing the release performance of the CA-TMZ nanofiber system.

Biphasic release was detected in all CA/TMZ nanofibers, with an initial burst followed by sustained release. The release within the first 8 hours for CA/TMZ5, CA/TMZ10, and CA/TMZ15 was measured at approximately 25%, 26%, and 22%, respectively. The initial burst seen in the first few hours (Hours 1-8) was likely due to the drug dissolving and diffusing from the nanofiber matrix into the surrounding environment. CA/TMZ10 exhibited the highest initial burst, while CA/TMZ15 had the lowest initial burst. It is expected that with higher drug concentration, the drug release percentage will be higher. However, at some point, the concentration would be saturated and aggregated, thus slowing the release rate. At higher concentrations, hydrophobic interactions between TMZ and CA also increased, causing the drug to adhere to the polymer matrix rather than diffuse out. From Hours 10 onwards, the release rate has slowed due to slower diffusion of the drug, as the concentration difference between the nanofiber and the surrounding medium decreases. The observed release profile aligns with the typical behavior of nanofiber-based drug delivery systems [23].

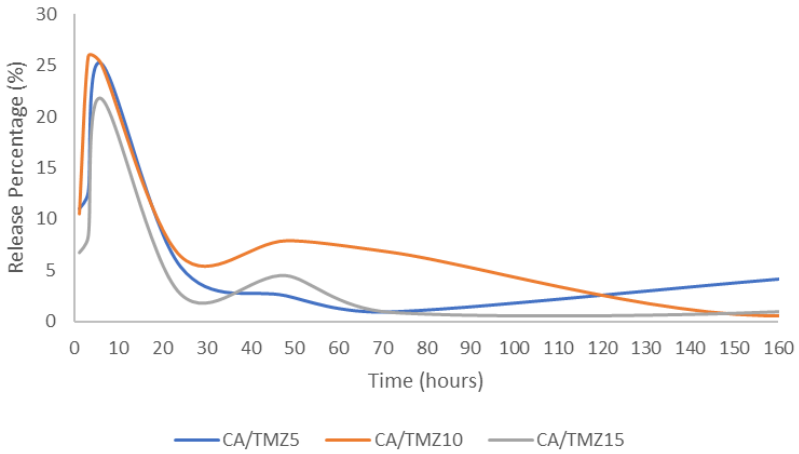

Figure 4. Drug release percentage of CA/TMZ nanofibers.

3.6. Cytotoxicity of CA/TMZ Extract

The bar graph in Figure 5 presents the cytotoxicity (%) over time (Day 1, 3, 5, 7) for electrospun CA nanofibers loaded with TMZ at different drug loadings (CA/TMZ5, CA/TMZ 10, and CA/TMZ15) as well as a drug-free control (CA). Over the course of study, CA consistently showed low toxicity (~5-15%). The drug-loaded groups (CA/TMZ5, CA/TMZ 10, and CA/TMZ15) exhibited increased cytotoxicity in terms of dose- and time-dependency. CA/TMZ5 showed a gradual increase in cell toxicity from ~28% on Day 1 to ~67% on Day 7. As the concentration of TMZ increased, cell toxicity also increased, with CA/TMZ10 and CA/TMZ15 exhibiting cytotoxicity of 52-86% and 71-83%, respectively. However,

on Day 7, CA/TMZ10 shows higher cytotoxicity than CA/TMZ1,5, despite its lower TMZ concentration, suggesting better sustained and effective delivery.

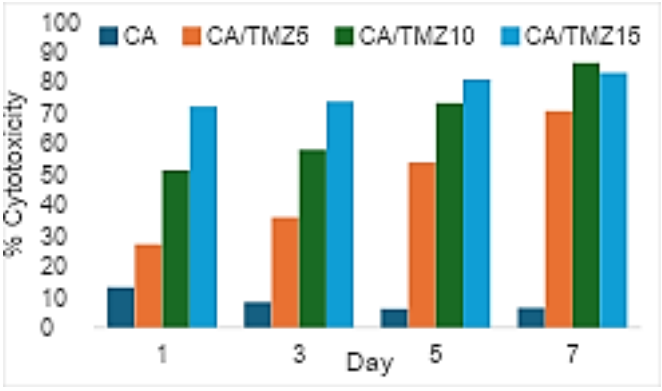

Figure 5. Cell toxicity of CA and CA/TMZ nanofibers.

4. DISCUSSION

The study demonstrates that CA nanofibers can serve as a viable matrix for sustained TMZ delivery. Electrospun fibers possessing a smooth surface, morphology with no defects, and controllable diameter have been made with the drug incorporated into them. Recent investigations have placed specific emphasis on the importance of electrospun fibers with uniform diameter and smooth surface propagation, relating these properties to improved performance of the resulting materials [24-25]. The increase in drug loading led to an increase in fiber thickness, which agrees with previous studies showing that drug incorporation can vary the viscosity and conductivity of a solution [26]. With respect to morphology, it was found that in the majority of the electrospun fibers, their cylindrical shape, random orientation, and interconnected porous structure were retained. These are the key attributes for effective drug delivery.

FTIR analysis was performed to assess the extent of unwanted bond formation and confirm the functional groups of the polymer-drug [27]. The presence of TMZ may influence molecular interactions that caused the OH stretching band to shift. This shift can indicate the change in the hydrogen-bonding network due to the encapsulation of TMZ into the CA matrix [19]. The addition of TMZ can also influence the surface hydrophobicity of the electrospun nanofibers. This was likely due to changes in surface chemistry and morphology caused by TMZ incorporation. The presence of hydrophilic functional groups on the fiber surface or the surface roughness may be altered by the addition of TMZ, thereby lowering the surface energy and enhancing water repellency. Similar trends have been observed in other electrospun polymer-based drug delivery systems, where higher drug loadings increased water contact angles due to diminished exposure of hydrophilic polymer and surface modifications [28]. High wettability can enhance water penetration, swelling, and drug diffusion, whereas a hydrophobic surface can permit slow drug release. By measuring the wettability, the drug release profile can be predicted and tailored [29].

To ensure structural integrity during surgical placement and residence within brain tissue, implantable systems need to undergo mechanical performance evaluation. The decrease in tensile modulus when TMZ concentration increased was likely due to the interference with polymer chain packing. This was due to a disruption of intermolecular hydrogen bonding within the CA matrix upon incorporation of the drug molecules. The reduction in tensile strength might be due to phase separation caused by poor TMZ dispersion, as defect formation during the electrospinning process can act as stress concentrators [21]. A tolerance without significant compromise can be observed in the CA matrix at low TMZ levels, as the 5 mg TMZ loading exhibited only a slight 2.21 MPa reduction in strength. Heterogeneity can also influence the ductility of electrospun nanofibers during drug distribution. At higher TMZ loading concentrations, polymer chain mobility may be restricted, or regions within the nanofiber structure may become brittle [30]. Although the mechanical properties decreased with TMZ loading, all samples remained within acceptable ranges for soft tissue implantation. The balance between mechanical support and drug-release efficiency can be ensured [31].

A desirable biphasic pattern was observed in the drug-release study. The result was consistent with prior reports on electrospun drug carriers, where the initial burst addresses the acute therapeutic needs, and release was maintained at therapeutic levels [32]. Over the 8 hours, the 22-26% release was suitable for short- to mid-term treatment windows, such as in the application of postoperative anti-tumor implants. Nanofibers were explored for their ability to control and sustain the release of active pharmaceutical ingredients, owing to the high surface area and fiber porosity. A previous study showed that drug release from nanofiber matrices was typically driven by a combination of diffusion and polymer degradation [23]. The rate of release was primarily influenced by the matrix composition and environmental factors, for example, pH and temperature. The initial burst release detected within the first few hours was a typical feature of nanofiber-based drug delivery systems. This can

be linked to the release of drug molecules from the surface or outer layer of the nanofibers. The release can be specifically controlled by modifying the fiber shape, the polymer molecular weight, and the amount of drug loaded into the nanofiber structure [33]. As the release progressed, the rate decreased, likely due to a reduction in the concentration gradient. Consistent with the previous study, the observed drug release over extended periods was attributable to continued diffusion of the drug through the fiber matrix [34].

In a cytotoxic study of the electrospun nanofibers, the results showed a sustained, controllable cytotoxic effect on GBM cells over 7 days. This addresses the limitation of conventional TMZ chemotherapy, in which the drug has a short half-life of 1.8 hours [35]. The electrospun nanofiber without the drug exhibited consistently low toxicity, confirming that CA nanofibers are non-toxic [36].

CONCLUSION

The results of this study showed the successful fabrication of electrospun CA nanofibers loaded with TMZ. The characterization of their structural, chemical, and drug-release properties was explored. Effective drug encapsulation, stable morphology, sustained release, and hydrophobic surface characteristics suitable for localized implantation were demonstrated. The structural integrity also supported the suitability of the electrospun nanofibers as implantable systems. Finally, the cytotoxic study has confirmed TMZ's ability to kill cancer cells. Overall, these findings support the potential application of CA/TMZ nanofibers as a controlled-release platform for glioblastoma therapy. In future work, the in vivo biocompatibility study, degradation behavior analysis, and long-term therapeutic efficacy in clinical settings can be explored.

ACKNOWLEDGMENTS

This work was supported by Universiti Teknologi Malaysia and the Ministry of Higher Education, Malaysia, under the Fundamental Research Grant Scheme (Grant no.: FRGS/1/2023/STG05/UTM/02/8).

REFERENCES

[1] A. A. Aly and M. K. Ahmed, "Nanofibers of cellulose acetate containing ZnO nanoparticles/graphene oxide for wound healing applications," *Int J Pharm*, vol. 598, p. 120325, Apr. 2021, doi: 10.1016/j.ijpharm.2021.120325.

[2] S. Yempally, S. M. Hegazy, A. Aly, K. Kannan, and K. K. Sadasivuni, "Non-Invasive Diabetic Sensor Based on Cellulose Acetate/Graphene Nanocomposite," *Macromol Symp*, vol. 392, no. 1, Aug. 2020, doi: 10.1002/masy.202000024.

[3] D. Atila, D. Keskin, and A. Tezcaner, "Cellulose acetate-based 3-dimensional electrospun scaffolds for skin tissue engineering applications," *Carbohydr Polym*, vol. 133, pp. 251–261, Nov. 2015, doi: 10.1016/j.carbpol.2015.06.109.

[4] R. J. Hickey and A. E. Pelling, "Cellulose Biomaterials for Tissue Engineering," *Front Bioeng Biotechnol*, vol. 7, Mar. 2019, doi: 10.3389/fbioe.2019.00045.

[5] A. Hiwrale, S. Bharati, P. Pingale, and A. Rajput, "Nanofibers: A current era in drug delivery system," *Heliyon*, vol. 9, no. 9, p. e18917, Sep. 2023, doi: 10.1016/j.heliyon.2023.e18917.

[6] M. K. Gaydhane, C. S. Sharma, and S. Majumdar, "Electrospun nanofibres in drug delivery: advances in controlled release strategies," *RSC Adv*, vol. 13, no. 11, pp. 7312–7328, 2023, doi: 10.1039/D2RA06023J.

[7] M. Hrubý, S. K. Filippov, and P. Štěpánek, "Smart polymers in drug delivery systems on crossroads: Which way deserves following?," *Eur Polym J*, vol. 65, pp. 82–97, Apr. 2015, doi: 10.1016/j.eurpolymj.2015.01.016.

[8] Y. Liu, S. Hao, L. Yu, and Z. Gao, "Long-term temozolomide might be an optimal choice for patients with multifocal glioblastoma, especially with deep-seated structure involvement: a case report and literature review," *World J Surg Oncol*, vol. 13, no. 1, p. 142, Dec. 2015, doi: 10.1186/s12957-015-0558-x.

[9] M. J. Ramalho, S. Andrade, M. Á. N. Coelho, J. A. Loureiro, and M. C. Pereira, "Biophysical interaction of temozolomide and its active metabolite with biomembrane models: The relevance of drug-membrane interaction for Glioblastoma Multiforme therapy," *European Journal of Pharmaceutics and Biopharmaceutics*, vol. 136, pp. 156–163, Mar. 2019, doi: 10.1016/j.ejpb.2019.01.015.

[10] R. Patil *et al.*, "Temozolomide Delivery to Tumor Cells by a Multifunctional Nano Vehicle Based on Poly(β-L-malic acid)," *Pharm Res*, vol. 27, no. 11, pp. 2317–2329, Nov. 2010, doi: 10.1007/s11095-010-0091-0.

[11] M. A. Wsoo *et al.*, "Vitamin D3-loaded electrospun cellulose acetate/polycaprolactone nanofibers: Characterization, in vitro drug release and cytotoxicity studies," *Int J Biol Macromol*, vol. 181, pp. 82–98, Jun. 2021, doi: 10.1016/j.ijbiomac.2021.03.108.

[12] M. Irani, G. M. M. Sadeghi, and I. Haririan, "The sustained delivery of temozolomide from electrospun PCL-Diol-b-PU/gold nanocompsite nanofibers to treat glioblastoma tumors," *Materials Science and Engineering: C*, vol. 75, pp. 165–174, Feb. 2017, doi: 10.1016/j.msec.2017.02.029.

[13] A. Ahad *et al.*, "Thermodynamic Solubility Profile of Temozolomide in Different Commonly Used Pharmaceutical Solvents," *Molecules*, vol. 27, no. 4, p. 1437, Feb. 2022, doi: 10.3390/molecules27041437.

[14] T. KODAWARA *et al.*, "Evaluation of Stability of Temozolomide in Solutions after Opening the Capsule," *YAKUGAKU ZASSHI*, vol. 129, no. 3, pp. 353–357, Mar. 2009, doi: 10.1248/yakushi.129.353.

[15] M. Arumugam, B. Murugesan, N. Pandiyan, D. K. Chinnalagu, G. Rangasamy, and S. Mahalingam, "Electrospinning cellulose acetate/silk fibroin/Au-Ag hybrid composite nanofiber for enhanced biocidal activity against MCF-7 breast cancer cell," *Materials Science and Engineering: C*, vol. 123, p. 112019, Apr. 2021, doi: 10.1016/j.msec.2021.112019.

[16] S. Absar, M. Khan, K. Edwards, and J. Neumann, "Investigation of synthesis and processing of cellulose, cellulose acetate and poly(ethylene oxide) nanofibers incorporating anti-cancer/tumor drug cis-diammineplatinum (II) dichloride using electrospinning techniques," *Journal of Polymer Engineering*, vol. 35, no. 9, pp. 867–878, Nov. 2015, doi: 10.1515/polyeng-2015-0057.

[17] C. D. L. Johnson, A. R. D'Amato, and R. J. Gilbert, "Electrospun Fibers for Drug Delivery after Spinal Cord Injury and the Effects of Drug Incorporation on Fiber Properties," *Cells Tissues Organs*, vol. 202, no. 1–2, pp. 116–135, 2016, doi: 10.1159/000446621.

[18] J. Du, E. Tan, H. J. Kim, A. Zhang, R. Bhattacharya, and K. J. Yarema, "Comparative evaluation of chitosan, cellulose acetate, and polyethersulfone nanofiber scaffolds for neural differentiation," *Carbohydr Polym*, vol. 99, pp. 483–490, Jan. 2014, doi: 10.1016/j.carbpol.2013.08.050.

[19] T. Sudiarti, D. Wahyuningrum, B. Bundjali, and I. Made Arcana, "Mechanical strength and ionic conductivity of polymer electrolyte membranes prepared from cellulose acetate-lithium perchlorate," *IOP Conf Ser Mater Sci Eng*, vol. 223, p. 012052, Jul. 2017, doi: 10.1088/1757-899X/223/1/012052.

[20] B. Li and X. Yang, "Rutin-loaded cellulose acetate/poly(ethylene oxide) fiber membrane fabricated by electrospinning: A bioactive material," *Materials Science and Engineering: C*, vol. 109, p. 110601, Apr. 2020, doi: 10.1016/j.msec.2019.110601.

[21] S.-F. Chou and K. A. Woodrow, "Relationships between mechanical properties and drug release from electrospun fibers of PCL and PLGA blends," *J Mech Behav Biomed Mater*, vol. 65, pp. 724–733, Jan. 2017, doi: 10.1016/j.jmbbm.2016.09.004.

[22] A. A. Razak, S. K. Masthanamma, B. Omshanthi, V. Suresh, and P. Obulamma, "Development and Validation of UV Method of Temozolomide in Bulk and Capsule Formulation," *Int J Pharm Sci Res*, vol. 4, no. 4, pp. 1419–1423, 2013.

[23] Y. Herdiana, N. Wathoni, S. Shamsuddin, and M. Muchtaridi, "Drug release study of the chitosan-based nanoparticles," *Heliyon*, vol. 8, no. 1, p. e08674, Jan. 2022, doi: 10.1016/j.heliyon.2021.e08674.

[24] M. Kwon, J. Kim, and J. Kim, "Photocatalytic Activity and Filtration Performance of Hybrid TiO2-Cellulose Acetate Nanofibers for Air Filter Applications," *Polymers (Basel)*, vol. 13, no. 8, p. 1331, Apr. 2021, doi: 10.3390/polym13081331.

[25] S. Majumder, A. Sharif, and M. E. Hoque, "Electrospun Cellulose Acetate Nanofiber: Characterization and Applications," in *Advanced Processing, Properties, and Applications of Starch and Other Bio-Based Polymers*, Elsevier, 2020, pp. 139–155. doi: 10.1016/B978-0-12-819661-8.00009-3.

[26] Y. Zhou, M. Wang, C. Yan, H. Liu, and D.-G. Yu, "Advances in the Application of Electrospun Drug-Loaded Nanofibers in the Treatment of Oral Ulcers," *Biomolecules*, vol. 12, no. 9, p. 1254, Sep. 2022, doi: 10.3390/biom12091254.

[27] F. N. Parın, Ç. İ. Aydemir, G. Taner, and K. Yıldırım, "Co-electrospun-electrosprayed PVA/folic acid nanofibers for transdermal drug delivery: Preparation, characterization, and in vitro cytocompatibility," *Journal of Industrial Textiles*, vol. 51, no. 1_suppl, pp. 1323S-1347S, Jun. 2022, doi: 10.1177/1528083721997185.

[28] Y. Hua *et al.*, "Poly(lactic-co-glycolic acid) microsphere production based on quality by design: a review," *Drug Deliv*, vol. 28, no. 1, pp. 1342–1355, Jan. 2021, doi: 10.1080/10717544.2021.1943056.

[29] R. Jiffrin *et al.*, "Electrospun Nanofiber Composites for Drug Delivery: A Review on Current Progresses," *Polymers (Basel)*, vol. 14, no. 18, p. 3725, Sep. 2022, doi: 10.3390/polym14183725.

[30] R. Ramachandran *et al.*, "Theranostic 3-Dimensional nano brain-implant for prolonged and localized treatment of recurrent glioma," *Sci Rep*, vol. 7, no. 1, p. 43271, Mar. 2017, doi: 10.1038/srep43271.

[31] M. Norouzi, "Recent advances in brain tumor therapy: application of electrospun nanofibers," *Drug Discov Today*, vol. 23, no. 4, pp. 912–919, Apr. 2018, doi: 10.1016/j.drudis.2018.02.007.

[32] Penabaka Venugopalaiah, KP Benidicts Prem Prakash, Yerikala Ramesh, and M Alagusundaram, "Formulation and evaluation of extended-release tablets of trimetazidine HCL," *World Journal of Advanced Research and Reviews*, vol. 18, no. 3, pp. 993–1002, Jun. 2023, doi: 10.30574/wjarr.2023.18.3.1003.

[33] A. M. Agiba *et al.*, "Advances in Light-Responsive Smart Multifunctional Nanofibers: Implications for Targeted Drug Delivery and Cancer Therapy," *Pharmaceutics*, vol. 16, no. 8, p. 1017, Jul. 2024, doi: 10.3390/pharmaceutics16081017.

[34] S. Wang *et al.*, "Improvement in the Sustained-Release Performance of Electrospun Zein Nanofibers via Crosslinking Using Glutaraldehyde Vapors," *Foods*, vol. 13, no. 10, p. 1583, May 2024, doi: 10.3390/foods13101583.

[35] M. Shamsipour, A. M. Mansouri, and P. Moradipour, "Temozolomide conjugated carbon quantum dots embedded in core/shell nanofibers prepared by coaxial electrospinning as an implantable delivery system for cell imaging and sustained drug release," *AAPS PharmSciTech*, vol. 20, no. 7, p. 259, Oct. 2019, doi: 10.1208/s12249-019-1466-0.

[36] T. P. M. Sunthar *et al.*, "Antibacterial Property of Cellulose Acetate Composite Materials Reinforced with Aluminum Nitride," *Antibiotics*, vol. 10, no. 11, p. 1292, Oct. 2021, doi: 10.3390/antibiotics10111292.